J Nanopart Res (2016) 18:314
DOI 10.1007/s11051-016-3581-0

RESEARCH PAPER

Systematic control of edge length, tip sharpness, thickness, and localized surface plasmon resonance of triangular Au nanoprisms

Yuta Noda · Tomokatsu Hayakawa

Received: 22 May 2016 / Accepted: 24 August 2016 / Published online: 22 October 2016

Abstract Triangular gold (Au) nanoprisms of various sizes were synthesized in a controlled way using a modified three-step seed-mediated method with different volumes of starting seed solution and subsequent first step's growth solution. The structures and optical properties of the triangular Au nanoprisms were investigated using transmission electron microscopy (TEM), atomic force microscopy, and UV–Vis–NIR spectrophotometry. The Au nanoprisms synthesized also varied in optical response frequency of localized surface plasmon resonance (LSPR) owing to electric dipole polarizations of the Au nanoprisms. This variation depended nonlinearly on the volume of the seed solution. From optical extinction spectra and careful TEM observations, the dipole LSPR peak frequency was found to be linearly proportional to the edge length of the Au nanoprisms. Consequently, it was experimentally shown that the LSPR optical response frequency of their colloidal solutions could be controlled in the near-infrared region (700–1200 nm), corresponding to an edge length of 40–180 nm of the Au nanoprisms. It was also demonstrated that the tip sharpness of triangular Au nanoprisms was improved by using fine Au seeds instead of coarse Au seeds, and the resulting Au nanoprisms were smaller and thinner. A formation mechanism of triangular Au nanoprisms shall also be discussed with a prospect of synthesizing very tiny Au nanoprisms.

Keywords Gold nanoprisms · Three-step seed-mediated method · Dipole polarization · Localized surface plasmon resonance · Near-infrared region · Edge length · Tip sharpness

Introduction

Metal nanoparticles have great potential to be used in optical, optoelectrical, and biological fields, owing to effects such as optical electric field enhancement (Xu et al. 2011; Schaadt et al. 2005), nonlinear ultrafast optics (Hayakawa et al. 2004; Tsutsui et al. 2011), and surface enhanced Raman scattering (SERS) (Haynes et al. 2005; Haes et al. 2005; Wang and Schlucker 2013), which can improve the efficiency of solar cell optical response, medical diagnosis, illuminations from light emitting diodes (LEDs), lasers, etc. This is in turn contributes to the growth of the active scientific field of plasmonics (Brongersma and Kik 2007; Maier and Atwater 2005). The effects mentioned above are produced by electric polarization of collective oscillations of free electrons localized in metal nanoparticles (Kreibig and Vollmer 1995) known as localized surface plasmon resonance

Electronic supplementary material The online version of this article (doi:10.1007/s11051-016-3581-0) contains supplementary material, which is available to authorized users.

Y. Noda · T. Hayakawa (✉)
Department of Frontier Materials, Field of Advanced Energy Conversion, Nagoya Institute of Technology, Gokiso, Showa, Nagoya 466-8555, Japan
e-mail: hayatomo@nitech.ac.jp

(LSPR). Recently, many researchers have focused on these interesting properties, and many papers on fundamental discoveries and device applications related to the optical properties of these nanoparticles (Eustis and El-Sayed 2006) have been published in rapid succession.

Electric polarization in metal nanoparticles varies depending on the shape and size of the nanoparticles, allowing researchers to realize a variety of LSPR properties. (Jain et al. 2006; Kelly et al. 2003; Lee and El-Sayed 2005). In addition, strong local fields are produced at the sharp portions of the tips and edges of rod-like particles and triangular nanoprisms (Liao and Wokaun 1982; Mohamed et al. 2000; Mahmoud and El-Sayed 2013; Shuford et al. 2005; Yang et al. 2009; Hao and Schatz 2004; Mohammadi et al. 2011; Lee et al. 2013). In particular, a unique nanoprism shape is expected to make it easy to be arrayed two dimensionally (Lee et al. 2013), which could further enhance the optical responses of the nanoprisms and be useful for practical applications.

To make progressive use of the LSPR properties of metal nanoprisms, optimal synthesis parameters must be determined in accordance with the shape, size, and, eventually, optical responses of the nanoprisms. Here, we focused ourselves on triangular gold (Au) nanoprisms and investigated a more controlled way to synthesize these nanoprisms with different edge lengths and thicknesses. Triangular metal nanoprisms are often accidentally produced in the presence of organic surfactants (Métraux and Mirkin 2005; Aherne et al. 2008; Goy-López et al. 2008; Guo et al. 2006; Shankar et al. 2004). In this study, we applied a very practical methodology for preferential synthesis of triangular Au nanoprisms, where a selective adsorption of iodide ions (I^-) on (111) planes of a cubic Au metal lattice occurred during a seed-mediated growth of Au nanometals (Millstone et al. 2008). We modified the method to alter the LSPR response in optical frequencies in an optimized way.

Experiments

Materials

Tetrachloroauric(III) acid trihydrate ($HAuCl_4 \cdot 3H_2O$), sodium borohydride ($NaBH_4$), cetyltrimethylammonium bromide (CTAB), L(+)-ascorbic acid, sodium hydroxide (NaOH), and sodium chloride (NaCl) were purchased from Kishida Chem. Co. Trisodium citrate [$Na_3(C_3H_5O(COO)_3)$] was provided by Kanto Chem. Co. Sodium iodide (NaI) was obtained from Nacalai Tesque.

Preparation of Au seed solution

1 ml of 10 mM $HAuCl_4$ and 1 ml of 10 mM trisodium citrate were added to 36 ml of Milli-Q water. 1 ml of 100 mM $NaBH_4$ stored in ice was added to the mixed solution with vigorous stirring. As a result, Au was reduced and the color of the solution changed from light yellow to wine red (see Scheme 1). We used different volumes of 10 mM trisodium citrate (between 1.0 and 1.4 ml) to vary the size of the Au seeds (Sau et al. 2001; Haiss et al. 2007).

Synthesis of Au nanoprisms

Millstone et al. (Millstone et al. 2005, 2008) reported that triangular Au nanoprisms could be synthesized using a three-step seed-mediated method. To do this, first, 150 ml of a 50 mM CTAB solution was prepared, and then a very small amount of NaI (50 μM I^- solution) was added to the CTAB solution. The presence of a small amount of I^- ions aided in the formation of the triangular Au nanoprisms. Growth solutions denoted as No. 1 and 2 (see Scheme 1) were prepared by adding 0.25 ml of 10 mM $HAuCl_4$ to 9 ml

Scheme 1 Three-step seed-mediated method with various volumes of the starting seed (*x*) and first step's growth solution (*y*). Resultant solutions are required to be filtered to collect Au nanoprisms after they have been rested for 30 min (see "Synthesis of Au nanoprisms" section for details)

of 50 mM CTAB solution, and then adding 0.05 ml of 10 mM ascorbic acid and 0.05 ml of 10 mM NaOH to the mixed solutions. The color of the solution changed from orange to colorless. The growth solution denoted as No. 3 was colorless and consisted of 250 ml of 10 mM $HAuCl_4$ and 90 ml of a 50 mM CTAB solution to which 0.5 ml of 10 mM ascorbic acid and 0.5 ml of 10 mM NaOH were added.

In the first step of the synthesis, x ml of the Au seed solution was gently stirred into growth solution No. 1 (Fan et al. 2010). Second, y ml of the first step's growth solution was added to solution No. 2 very quickly (within 3–5 s). Finally, all of the second step's growth solution was added to solution No. 3 quickly (within 3–5 s) and the resulting solution was transferred to a refrigerator as soon as possible to rest for 30 min. After the third growth step, the resultant solution changed from colorless to deep magenta purple.

The colloidal solution contained not only Au nanoprisms but also a small amount of spherical Au nanoparticles. To separate the two types of particles, the solution was centrifuged at $2100\times g$ for 1 min, after adding NaCl and keeping the solution for at least 1 h (Young et al. 2012). As NaCl was added, the ionic strength of the solution increased, and Au nanoprisms aggregated owing to their inter-planar interactions. After the liquid at the top of the container was removed, the aggregates were re-immersed in a 50 mM CTAB solution to separate aggregated Au nanoprisms, because the re-immersed solution contained less NaCl, and the inter-planar interactions of the Au nanoprisms were consequently weaker. Thus, the Au nanoprisms were no longer aggregated and exhibited a green color (See a picture in Scheme 1, which shows an example of the Au nanoprisms solution synthesized when $x = 1.0$ and $y = 1.0$ ml).

Characterizations

The optical extinction spectra of the resultant colloidal solutions were analyzed with a UV–Vis–NIR spectrophotometer (JASCO, V-670). The morphologies and thicknesses of the Au nanoprisms were analyzed using transmission electron microscopy (TEM) (JEOL, JEM-2010) and atomic force microscopy (AFM) (DFM mode, SPA-300HV/SPI4000, Seiko Instruments Inc.), respectively. For the statistical analysis of the edge length and tip sharpness, we took about ten TEM images so that each of them included several tens of prisms. Then, we randomly picked up 80 prisms for the statics. As for AFM data, we took a couple of AFM images, each of which included more than ten prisms and we picked up 10 of them for the estimation of the averaged thickness and error bars.

Results and discussion

Influence of the Au seed solution volume

Figure 1 shows optical extinction spectra and the LSPR peak positions of Au nanoprism colloidal solutions synthesized with various volumes of the starting Au seed solution (x) with fixed y (=1.0 ml). The spectra are composed of a strong broadband at long wavelengths, owing to the electric dipole polarization (D) of the LSPR of Au nanoprisms, and a small peak on the hump of the dipole LSPR band, which is due to the quadrupole polarization (Q) of the Au nanoprisms. (Millstone et al. 2005) A peak located at $\sim$530 nm is attributed to residual spherical Au nanoparticles. It was found that the dipole LSPR peak positions of the Au nanoprisms shifted to shorter wavelengths (from 1100 to 800) with increasing

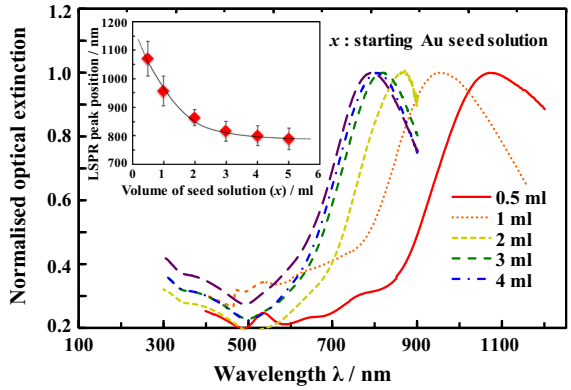

Fig. 1 Optical extinction spectra of triangular Au nanoprisms synthesized with various volumes of the starting Au seed solution (x) with 1.0 ml trisodium citrate solution (referred to as "coarse" Au seeds), where the first step's growth solution volume is fixed as $y = 1.0$ ml. The dipole LSPR peak position (D) is shifted to shorter wavelengths with increasing x. The hump of the dipole LSPR band is assigned to quadrupole polarization (Q) of the Au nanoprisms. The *inset* shows the dipole LSPR peak position as a function of the volume of the starting seed solution (x). The degree of the shift reduces at higher seed solution volumes ($x \geq 3$)

volume of the Au seed solution x. As shown in the inset of Fig. 1, the higher volume of the seed solution resulted in a smaller shift of the LSPR peak position, indicating a nonlinear dependence of the LSPR peak wavelength on x.

The spherical Au nanoparticles were formed as by-product in this synthesis method, but they could easily be removed by centrifugation because Au nanoprisms were agglomerated into cluster after NaCl addition [the spectra shown in Fig. 1 were obtained as those of redistributed Au nanoprisms after centrifugation (See also the section "Synthesis of Au nanoprisms" in "Experiments")]. Nevertheless, a certain amount of Au nanospheres indeed remained even after centrifugation. One of the possible reasons is that Au nanospheres might be trapped in the cluster of Au nanoprisms. It is supposed that larger Au nanoprisms, which were synthesized with lower Au seed volume, were easy to trap Au nanospheres in the cluster of Au nanoprisms, resulting in higher residual Au nanospheres, as indicated with the peak at 530 nm for 0.5 ml Au seed solution in Fig. 1.

Figure 2 shows TEM images and the size distributions of Au nanoprisms synthesized in different volumes of the seed solution (x), as well as a typical electron diffraction (ED) pattern. The red square marker in the ED pattern (Fig. 2b) highlights one of the bright spots indicative of the {111} plane of the Au nanoprisms, and the yellow circle marker highlights one of the weak spots considered to indicate the $\frac{1}{3}\{\bar{4}22\}$ plane derived from the local hexagonal-like structure observable only for noble metal nanoplates, that are atomically flat and have the presence of stacking faults/twins on (111) planes (Jin et al. 2001; Tsuji et al. 2006; Kirkland et al. 1990). This ED pattern provides evidence that the triangular-shaped Au nanoprisms synthesized were single crystals and the top flat surface was normal to {111} planes. The TEM images show that triangular Au nanoprisms and hexagonal Au nanoplates coexisted. The edge lengths of the Au nanoprisms were analyzed from the TEM images and found to decrease with increasing seed solution volume x. And, also many nanoprism tips were observed to be rounded. Figure 2i shows the change in mean edge length of Au nanoprisms as a function of the volume of the seed solution x. The edge lengths of Au nanoprisms varied from 180 to 80 nm with a narrow size distribution (see inset histograms in Fig. 2). Using the results shown in the inset of Figs. 1 and 2i, a relationship between the LSPR peak position and the mean edge length of the Au nanoprisms is derived, as shown in Fig. 3, which shows that the LSPR peak positions are linearly proportional to the edge length of the Au nanoprisms in the size range of 75–120 nm. However, for Au nanoprisms with an edge length greater than 150 nm, the LSPR peak position tends to be saturated. From later AFM data, we believe the saturation is because the triangular Au nanoprism thickness was increased to $\sim$15 nm while it was kept almost constant ($\sim$11 nm) for the region of 75–120 nm. Another possibility is related to the tip sharpness of the Au nanoprisms. As shown in the next section, the radius of the tip curvature becomes larger as the Au nanoprism edge length increases [the "snipping effect" (Shuford et al. 2005)].

Control of Au seed size and resultant triangular Au nanoprisms

To investigate the effect of Au seed size, we prepared fine Au seeds by adding excess trisodium citrate, which is a protective agent of Au seeds (Sau et al. 2001; Haiss et al. 2007) (see "Experiments" section). Figure 4 shows optical extinction spectra of Au "seed" colloidal solutions synthesized with three different volumes of trisodium citrate solution (1.0, 1.2, and 1.4 ml). The inset of Fig. 4 shows the LSPR peak position of Au spherical seeds in the seed solution. By adding more trisodium citrate, the LSPR peak position around 510 nm was shifted to shorter wavelengths. Figure 5 shows TEM images and size distributions of the seed solutions. The mean seed diameter was determined to be about 10 nm with a standard deviation of 1.56 nm when 1.0 ml of trisodium citrate was added, while the addition of 1.4 ml of trisodium citrate resulted in a mean diameter of 3.8 nm with a standard deviation of 0.7 nm. Very fine Au seeds with a smaller standard deviation (SD) can be obtained by adding excess trisodium citrate. Figure 6 shows TEM images of the resultant Au nanoprisms synthesized with $x' = 1.0$ ml of very fine Au seed solution (Fig. 6a) (1.4 ml of sodium citrate solution) and those of Au nanoprisms synthesized with the corresponding volume of coarse Au seed solution (Fig. 6b) (1.0 ml of sodium citrate solution). The use of fine Au seeds improves the sharpness of the

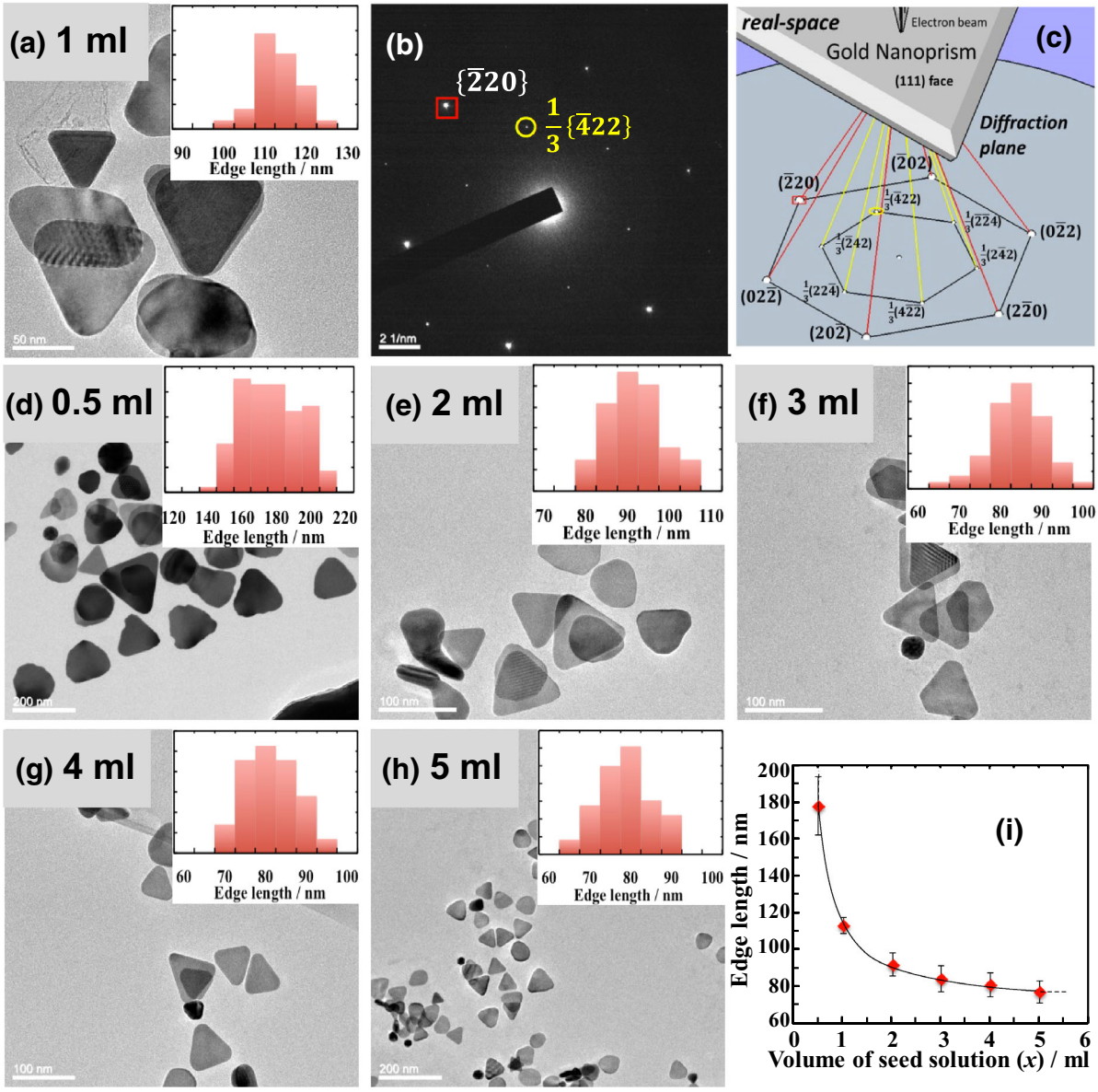

Fig. 2 TEM images and electron diffraction pattern of Au nanoprisms synthesized with various volumes of seed solution (x). *Insets* show the size distribution of the Au nanoprisms. In **b**, **c**, the *red square* highlights one of the strong spots in the diffraction pattern showing the {111} plane of Au nanoprisms and the inner *yellow circle* highlights one of the weak spots that is considered to be indicating the $\frac{1}{3}$ {$\bar{4}$22} plane. Most nanoprism edges are rounded. In **i**, the edge length of Au nanoprisms synthesized with various volumes of the starting seed solution (x) is shown to vary from 180 to 80 nm

resultant Au nanoprism tips, as shown in Table 1. Hence, it is expected that the Au nanoprisms exhibit stronger local fields near the tips of the triangles (Yamaguchi et al. 2007). Regardless of the Au seed solution volume, finer Au seeds resulted in sharper Au nanoprisms tips (compare (c) and (d) in Fig. 6, and see also Table 1; 26.9 → 18.7 nm for 0.5, 16.8 → 7.9 nm for 1.0 ml). However, their distribution (percentage error) was still large as to be 30.1 % (26.9 ± 8.1 nm), 37.4 % (18.7 ± 7.0 nm), 23.8 % (16.8 ± 4.0 nm) and 25.3 % (7.9 ± 2.0 nm), respectively, for 0.5 ml coarse, 0.5 ml fine, 1.0 ml coarse

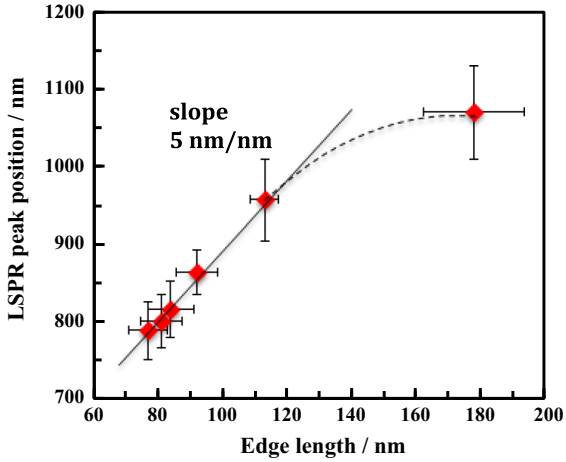

Fig. 3 Relationship between LSPR peak positions and edge length of the Au nanoprisms synthesized with coarse Au seeds (trisodium citrate solution: 1.0 ml), where the starting seed solution x was varied from 0.5 to 4.0 ml and the volume of the first step's growth solution y was fixed at 1.0 ml

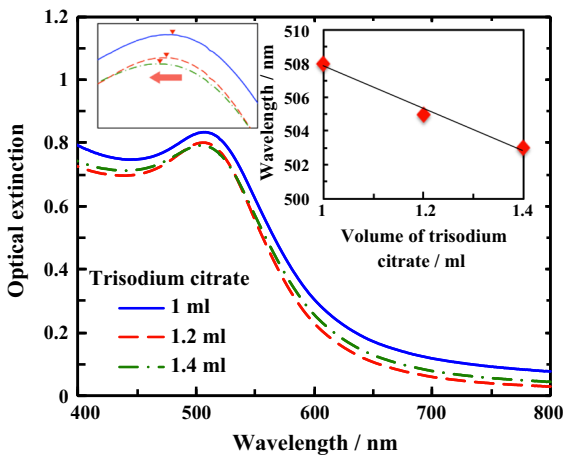

Fig. 4 Extinction spectra of Au seed solution synthesized with various volume of trisodium citrate. The *inset* on the *left* displays an enlarged image of the peaks. The *inset* on the *right* shows the relationship between the LSPR peak positions of Au seed solutions and the volume of trisodium citrate

and 1.0 ml fine seeds. Nevertheless, the higher volume of seed solution regardless of fine/coarse seeds improved the statistical distribution of tip curvature radius, which can be correlated with being the narrower distribution of edge length [8.8 % (177.4 ± 15.7 nm) → 4.0 % (113.3 ± 4.5 nm) for coarse seeds, 10.2 % (179.1 ± 18.2 nm) → 8.6 % (106.1 ± 9.1 nm) for fine seeds]. On the other hand, the smaller volume of fine Au seed solution (0.5 ml) resulted in larger Au nanoprisms, as also seen in Table 1, together with less irregular-shaped Au nanoparticles, including hexagonal and spherical nanoparticles (see Fig. S1 in Supporting Information).

Influence of the volume of the first step's growth solution

To synthesize smaller Au nanoprisms having dipole LSPR in the shorter wavelength region, we attempted to change the volume ($0.5 \leq y \leq 3.0$ ml) of solution No. 1 with Au seeds (see Scheme 1), called the first step's growth solution, when starting with very fine Au seeds ($x' = 5.0$ ml). Figure 7a, b shows optical extinction spectra of Au nanoprisms synthesized with various volumes of the starting seed solution x' (with the y value fixed as 1.0 ml) and the subsequent first step's growth solution y (with the x' value fixed to be 5.0 ml) with very fine Au seeds, respectively. Figure 7c shows the dipole LSPR peak positions of the Au nanoprisms synthesized as a function of the volumes of the respective solutions. The LSPR peak positions of the colloidal solutions were shifted to shorter wavelengths (from 1200 to 700 nm), and nonlinear behaviors were observed for the respective synthesis routes. Furthermore, as seen in Fig. 7a, the Au nanoprisms synthesized with 0.5 ml fine Au seed solution exhibited a broader bandwidth with a peak near 1000 nm, which is due to the presence of different morphologies (hexagonal/spherical, snipped) of Au nanoprisms (see Fig. 6c). Figure S1 (Supporting information) shows the corresponding TEM images and size distributions of Au nanoprisms synthesized with various volumes of the starting fine Au seed solution (x') and the subsequent first step's growth solution (y). The complied data are shown in Fig. 8, which shows a dependence of the volumes of the respective solutions (from 0.5 to 5.0 ml) on the edge length of the synthesized Au nanoprisms. The edge length of Au nanoprisms varied from 180 to 40 nm depending on the volume of the seed solution ($0.5 \leq x' \leq 5.0$, $y = 1.0$ ml) or first step's growth solution ($0.5 \leq y \leq 2.5$, $x' = 5.0$ ml). However, after excessive addition of the first step's growth solution ($y \geq 3.0$ ml), it was difficult to separate Au nanoprisms and spherical particles. In the corresponding LSPR spectrum (Supporting information Fig. S2 for $y = 3.0$ ml), Au nanoprisms were not clearly confirmed and only a very small amount of Au nanoprisms

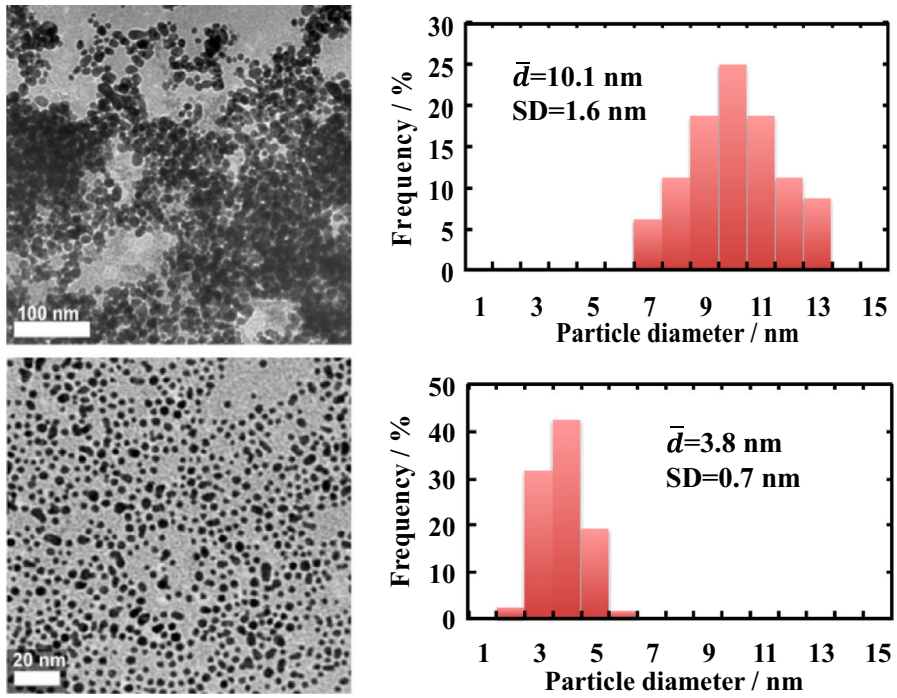

Fig. 5 TEM images of Au seeds synthesized with (*upper*) 1 and (*lower*) 1.4 ml trisodium citrate. By adding excess trisodium citrate, the average seed size changes from 10 to 3.8 nm, with a very small standard deviation (SD)

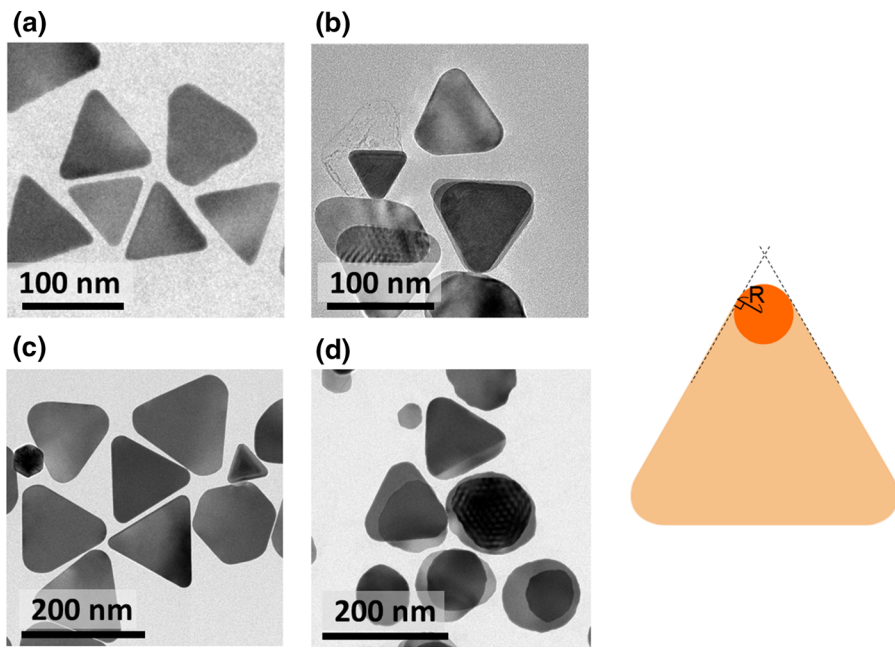

Fig. 6 TEM images of triangular Au nanoprisms synthesized with **a** 1.0 ml fine seed solution, **b** 1.0 ml coarse seed solution, **c** 0.5 ml fine seed solution, and **d** 0.5 ml coarse seed solution. The use of very fine Au seeds improved the sharpness of edges and tips. The data for averaged edge length and tip curvature *R* of Au nanoprisms obtained are listed in Table 1

was observed using TEM (see also Fig. S1). It was because Au nanoprisms synthesized with excessive *y* volume had weak inter-planar interactions even with the aid of NaCl (see the purification process in "Synthesis of Au nanoprisms" section). To see the relationship between the edge length and LSPR peak

Table 1 Mean edge length and tip curvature radius of Au nanoprisms synthesized with coarse (10 ± 1.6 nm) and fine (3.8 ± 0.7 nm) Au seeds

	Mean edge length (nm)	Mean tip curvature radius, R (nm)
0.5 ml coarse seed solution	177.4 ± 15.7	26.9 ± 8.1
0.5 ml fine seed solution	179.1 ± 18.2	18.7 ± 7.0
1.0 ml coarse seed solution	113.3 ± 4.5	16.8 ± 4.0
1.0 ml fine seed solution	106.1 ± 9.1	7.9 ± 2.0

Systematic control of the edge length of Au nanoprisms and localized surface plasmon resonance frequency

position of the Au nanoprisms, the results of Figs. 7c and 8 were combined and are shown in Fig. 9, which reveals that the dipole LSPR peak positions are also linearly proportional to the edge length of Au nanoprisms when fine Au seeds are used.

In relation to a picture in Scheme 1, it can be mentioned that a low volume of Au seeds (0.5 and 1.0 ml) resulted in green color of Au nanoprism solution, which means the longer LSPR wavelength of large Au nanoprisms. To shorten LSPR wavelength of Au nanoprisms, a higher volume of Au seeds (x') is needed, as shown in Fig. 8. Further adjustment of the first step's growth solution in volume (y) can shorten LSPR wavelength, resulting in blue coloration, although LSPR wavelength (or edge length) has a tendency to be saturated.

Thickness of Au nanoprisms

Figure S3 (Supporting information) depicts AFM images and height profiles of typical Au nanoprisms synthesized with coarse and fine Au seeds (Fig. 5). When $x' = 5.0$ ml (fine Au seeds) and $y < 3.0$ ml, the resultant Au nanoprisms have a thickness $t < 5$ nm. Figure 10 shows changes in the thickness of Au nanoprisms synthesized with coarse or fine Au seeds. When coarse Au seeds (∼10 nm) were used, Au nanoprisms with less than 10 nm thickness no longer existed. However, when fine Au seeds (∼3.8 nm) were used, it was possible to obtain tiny Au nanoprisms with thicknesses almost the same as the diameter of the fine Au seeds (about 4 nm). The use of very fine Au seeds allowed us to obtain triangular Au nanoprisms with sharp tips, shorter edge lengths, and lesser thicknesses of ∼4 nm, and their dipole LSPR could be controlled from 700 to 1200 nm.

Discussion

Because the series of Au nanoprisms on line A in Fig. 9 (LSPR wavelength vs. edge length), which was synthesized with the different volumes of the first step's growth solution (y) with fine Au seeds (3.8 ± 0.7 nm), had a constant thickness of ∼4 nm (see Fig. 10), the LSPR variation was solely caused by variation in the edge length of the Au nanoprisms. On the contrary, the LSPR frequency of Au nanoprisms synthesized with a varied volume (x') of the fine Au seeds was monotonically dependent on both thickness (see Fig. 10) and edge length (see line B in Fig. 9). For coarse Au seeds (10.1 ± 1.6 nm), we observed a linear dependence of dipole LSPR wavelength on the edge length of the resultant Au nanoprisms: a slope of 5 nm/nm (see Fig. 3), which increased to 15 nm/nm (line A in Fig. 9) when fine Au seeds were used. Because the thicknesses of the Au nanoprisms were a constant of ∼12 and ∼4 nm for coarse and fine Au seeds, respectively (see Fig. 10), the difference in the slopes is attributed to the sharpness of Au triangular nanoprism tips, or "snipping" effects (Shuford et al. 2005). Moreover, the slope of line B in Fig. 9 decreased to 3.1 nm/nm, where the thickness was linearly varied with the edge length at the same time (see Fig. 10). Thus, thicker Au nanoprisms with a constant edge length were considered to exhibit shorter LSPR wavelength, as in the computational results (Shuford et al. 2005).

From a practical point of view, the results obtained in the present work are convincing because they are supported by the statistical data of many TEM and AFM images. Our synthesis methodology revealed that the thickness of the synthesized Au nanoprisms was highly influenced by the starting size of the Au seeds and the initial growth of Au seeds in solution No. 1 added with the starting seed solution. The edge

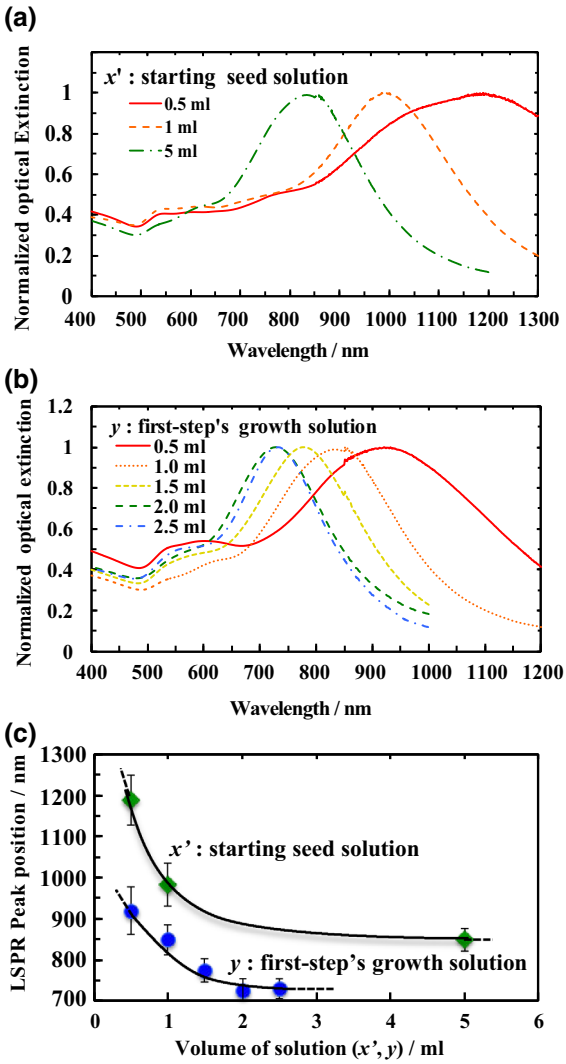

Fig. 7 **a**, **b** Extinction spectra of triangular Au nanoprisms synthesized with various volumes of the starting seed solution x' (with y fixed as 1.0 ml) and the first step's growth solution y (with x' fixed as 5.0 ml) from fine Au seeds. **c** Relationship between dipole LSPR peak positions and volumes of the fine starting seed solution ($0.5 \leq x \leq 5.0$; $y = 1.0$ ml) and the first step's growth solution ($0.5 \leq y \leq 2.5$; $x' = 5.0$ ml). Dipole LSPR peaks vary from 700 to 1200 nm

length of the Au nanoprisms could independently be controlled with the volume of the first step's growth solution.

Moreover, our results demonstrated that the Au seeds used in the early stage of the synthesis are key to controlling synthesis of Au nanoprisms. Practically, the final size of synthesized Au nanoprisms nonlinearly depended on the concentration of the starting and

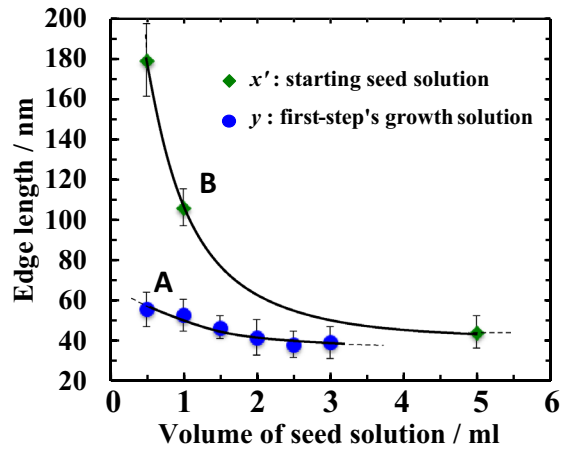

Fig. 8 Size distribution of Au nanoprisms synthesized with various volumes of the fine starting seed solution ($0.5 \leq x' \leq 5.0$; $y = 1.0$ ml) and the first step's growth solution ($0.5 \leq y \leq 3.0$; $x' = 5.0$ ml). Edge lengths of Au nanoprisms varied from 40 to 180 nm

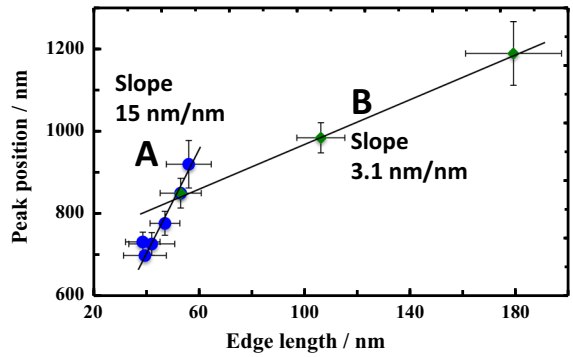

Fig. 9 Relationship between dipole LSPR peak positions and edge length of Au nanoprisms synthesized with fine Au seeds. The data on *line A* were with obtained with $x' = 5.0$ and $0.5 \leq y \leq 3.0$ ml, while the data on *line B* were obtained with $0.5 \leq x' \leq 5.0$ and $y = 1.0$ ml

grown seeds in the initial and first growth step, respectively, and the former influenced not only the edge length but also the thickness of the synthesized Au nanoprisms. Coarse Au seeds exhibited a large volume with a broad size dispersion (see Fig. 5), indicating that they were not suitable for the well-balanced growth of Au nanoprisms. Fine Au seeds ($\sim$3.8 nm in this study) were indispensable in obtaining sharper Au nanoprisms tips, and the edge length and thickness of the Au nanoprisms were determined to be sensitive to the volume of the starting seed solution. Thin Au nanoprisms, whose edge length

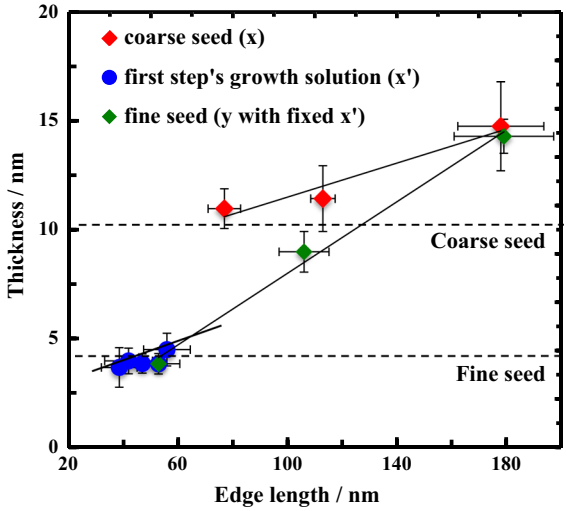

Fig. 10 Change in thickness of Au nanoprisms synthesized with coarse (10 ± 1.6 nm) and fine (3.8 ± 0.7 nm) Au seeds analyzed with AFM. *Dotted lines* show coarse (*upper*) and fine seed (*lower*) diameters. Using coarse seeds, nanoprisms less than 10 nm *thick* no longer existed. However, using fine Au seeds, the Au nanoprisms had *thicknesses* almost the same as the fine seed diameter

was controllable by the volume of the first step's growth solution to some extent, could be synthesized in a large volume of the starting solution ($x' \geq 5$ ml).

Although there were included many Na^+ ions in the growth and resultant solutions, they had no remarkable effects on the growth of the Au nanoprisms except for the change in the ionic strength after the growth step. Millstone et al. (2008) tried to use LiI, KI and NaI as iodide ion sources and reported that Au nanoprisms could be synthesized using any iodide source.

It proved difficult to synthesize further tiny nanoprisms with shorter dipole LSPR wavelength by controlling the starting seed solution, because a larger volume of the seed solution ($x' \gg 5$ ml) was required. In contrast, by changing the volume of the first step's growth solution, tinier Au nanoprisms were more easily obtained (see Fig. 8). Therefore, by appropriate combination of the volumes of the starting seed and first step's growth solutions, it is possible to control the size (edge length) of Au nanoprisms and resultantly dipole LSPR frequency. It should be also noted that the thickness of Au nanoprisms was dependent on the volume and size of the starting seed solution.

The formation mechanism of Au nanoprisms can be explained as follows: In the presence of a very small amount of iodide ions, iodide ions were attached to the $(111)_{fcc}$ planes of Au, and CTAB combined with iodide ions and arrayed on the $(111)_{fcc}$ planes selectively. As a result, the growth of Au in the [111] direction was prevented (see Scheme 2) (Ha et al. 2007). The edge length of triangular Au nanoprisms could be varied by the seed concentrations in the growth solutions (Fan et al. 2010). Recently, Ah et al. (2005) reported synthesis of Au nanoprisms (nanoplates) where polyvinylpyrrolidone (PVP) was used as a protective agent and LSPR wavelength was varied from 700 to 2000 nm. Our approach, in which CTAB was used as a protective agent for Au (111) planes, can also be applied to synthesize larger Au nanoprisms with ~2000 nm LSPR, but this work has here been focused on the effects of the seed conditions on the fined corner sharpness and of the volumes of seed/-growth solutions on the edge length and LSPR wavelength of Au nanoprisms. As the seed concentration in the growth solutions was reduced, the amount of Au^- ions used for the growth of each Au nanoprism was increased and growth step of the Au prisms became dominant (see Scheme 3). At present, despite the aforementioned better understanding and well-controlled methodology, synthesis of tiny Au nanoprisms smaller than 40 nm with good sharpness in liquid phase is still challenging, because the growth step of Au nanoprisms has to be more restricted and finer starting Au seeds are required.

Conclusions

In this paper, we demonstrated control of the morphology (edge length, thickness, and tip sharpness) and LSPR frequency of triangular Au nanoprisms by using various volumes of the starting and first step's

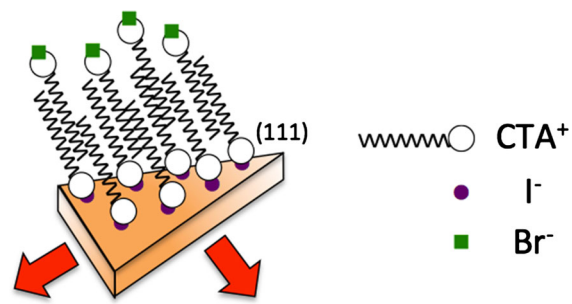

Scheme 2 Mechanism of Au nanoprism formation with a small amount of iodide ions (Ha et al. 2007)

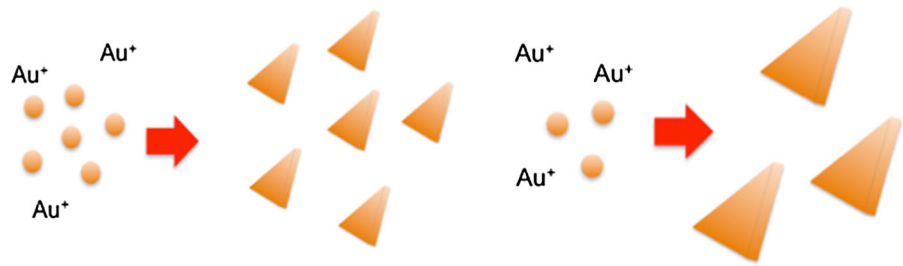

Scheme 3 Mechanism of size control of Au nanoprisms by changing the volume of the starting seed solution (Fan et al. 2010)

growth seed solutions with an easy and low-cost synthesis method. The nanoprism's edge length could be controlled from 180 to 40 nm, and LSPR wavelength could be tuned from 1200 to 700 nm. We were able to improve the sharpness of the tips and obtain thinner nanoprisms ($t \approx 4$ nm) by using fine Au seeds.

Acknowledgments This work was supported by the JSPS International Training Program (ITP), "Young Scientist-Training Program for World Ceramics Networks" and by a grant from Institute of Ceramics Research and Education (ICRE) in Nagoya Institute of Technology.

References

Ah CS, Yun YJ, Park HJ, Kim WJ, Ha DH, Yun WS (2005) Size-controlled synthesis of machinable single crystalline gold nanoplates. Chem Mater 17:5558–5561. doi:10.1021/cm051225h

Aherne D, Ledwith DM, Gara M, Kelly JM (2008) Optical properties and growth aspects of silver nanoprisms produced by a highly reproducible and rapid synthesis at room temperature. Adv Funct Mater 18:2005–2016. doi:10.1002/adfm.200800233

Brongersma ML, Kik PG (2007) Surface plasmon nanophotonics, Springer series in optical sciences. Springer, Berlin

Eustis S, El-Sayed MA (2006) Why gold nanoparticles are more precious than pretty gold: noble metal surface plasmon resonance and its enhancement of the radiative and nonradiative properties of nanocrystals of different shapes. Chem Soc Rev 35:209–217. doi:10.1039/B514191E

Fan X, Guo ZR, Hong JM, Zhang Y, Zhang JN, Gu N (2010) Size-controlled growth of colloidal nanoplates and their high-purity acquisition. Nanotechnology 21:105602/1-7. doi:10.1088/0957-4484/21/10/105602

Goy-López S, Castro R, Taboada P, Mosquera V (2008) Block copolymer-mediated synthesis of size-tunable gold nanospheres and nanoplates. Langmuir 24:13186–13196. doi:10.1021/la802279j

Guo Z, Zhang Y, Mao Y, Huang L, Gu N (2006) Synthesis of microsized gold nanoplates by a self-seeding method in ethanol solution. Mater Lett 60:3522–3525. doi:10.1016/j.matlet.2006.03.043

Ha TH, Koo HJ, Chung BH (2007) Shape-controlled syntheses of gold nanoprisms and nanorods influenced by specific adsorption of halide ion. J Phys Chem 111:1123–1130. doi:10.1021/jp066454l

Haes AJ, Haynes CL, McFarland AD, Schatz GC, Van Duyne RP, Zou S (2005) Plasmonic materials for surface-enhanced sensing and spectroscopy. MRS Bull 30:368–375. doi:10.1557/mrs2005.100

Haiss W, Thanh NTK, Aveyard J, Fernig DG (2007) Determination of size and concentration of gold nanoparticles from UV–Vis spectra. Anal Chem 79:4215–4221. doi:10.1021/ac0702084

Hao E, Schatz GC (2004) Electromagnetic fields around silver nanoparticles and dimers. J Chem Phys 120:357–366. doi:10.1063/1.1629280

Hayakawa T, Usui Y, Bharathi S, Nogami M (2004) Second harmonic generation from coupled surface plasmon resonances in self-assembling gold nanoparticles monolayer coated with an aminosilane. Adv Mater 16:1408–1412. doi:10.1002/adma.200306463

Haynes CL, McFarland AD, Van Duyne RP (2005) Surface-enhanced Raman spectroscopy. Anal Chem 77:338A–346A. doi:10.1021/ac053456d

Jain PK, Lee KS, El-Sayed IH, El-Sayed MA (2006) Calculated absorption and scattering properties of gold nanoparticles of different size, shape, and composition: applications in biological imaging and biomedicine. J Phys Chem B 110:7238–7248. doi:10.1021/jp057170o

Jin R, Cao YW, Mirkin CA, Kelly KL, Schatz GC, Zheng JG (2001) Photoinduced conversion of silver nanospheres to nanoprisms. Science 294:1901–1903. doi:10.1126/science.1066541

Kelly KL, Coronado E, Zhao LL, Schatz GC (2003) The optical properties of metal nanoparticles: the influence of size, shape, and dielectric environment. J Phys Chem B 107:668–677. doi:10.1021/jp026731y

Kirkland AI, Edwards PP, Jefferson DA, Duff DG (1990) The structure, characterization, and evolution of colloidal metals. Annu Rep Prog Chem Sect C: Phys Chem 87:247–304. doi:10.1039/PC9908700247 **(Chapter 8)**

Kreibig U, Vollmer M (1995) Optical properties of metal clusters, Springer series in materials science. Springer, Berlin

Lee KS, El-Sayed MA (2005) Dependence of the enhanced optical scattering efficiency relative to that of absorption for gold metal nanorods on aspect ratio, size, end-cap shape, and medium refractive index. J Phys Chem B 109:20331–20338. doi:10.1021/jp054385p

Lee YH, Lee CK, Tan B, Tan JMR, Phang IY, Ling XY (2013) Using the Langmuir–Schaefer technique to fabricate large-area dense SERS-active Au nanoprism monolayers films. Nanoscale 5:6404–6412. doi:10.1039/c3nr00981e

Liao PF, Wokaun A (1982) Lightning rod effect in surface enhanced Raman scattering. J Phys Chem 76:751–752. doi:10.1063/1.442690

Mahmoud MA, El-Sayed MA (2013) Efferent plasmon sensing behavior of silver and gold nanorods. J Phys Chem Lett 4:1541–1545. doi:10.1021/jz4005015

Maier SA, Atwater HA (2005) Plasmonics: localization and guiding of electromagnetic energy in metal/dielectric structures. J Appl Phys 98:011101/1-10. doi:10.1063/1.1951057

Métraux GS, Mirkin CA (2005) Rapid thermal synthesis of silver nanoprisms with chemically tailorable thickness. Adv Mater 17:412–415. doi:10.1002/adma.200401086

Millstone JE, Park S, Shuford KL, Qin L, Schatz GC, Mirkin CA (2005) Observation of a quadrupole plasmon mode for a colloidal solution of gold nanoprisms. J Am Chem Soc 127:5312–5313. doi:10.1021/ja043245a

Millstone JE, Wei W, Jones MR, Yoo H, Mirkin CA (2008) Iodide ions control seed-mediated growth of anisotropic gold nanoparticles. Nano Lett 8:2526–2529. doi:10.1021/nl8016253

Mohamed MB, Volkov V, Link S, El-Sayed MA (2000) The 'lightning' gold nanorods: fluorescence enhancement of over a million compared to the gold metal. Chem Phys Lett 317:517–523. doi:10.1016/S0009-2614(99)01414-1

Mohammadi R, Unger A, Elmers HJ, Schonhense G, Shushtari MZ, Kreiter M (2011) Manipulating near field polarization beyond the diffraction limit. Appl Phys B 104:65–71. doi:10.1007/s00340-011-4475-6

Sau TK, Pal A, Jana NR, Wang ZL, Pal T (2001) Size controlled synthesis of gold nanoparticles using photochemically prepared seed particles. J Nanopart Res 3:257–261. doi:10.1023/A:1017567225071

Schaadt DM, Feng B, Yu ET (2005) Enhanced semiconductor optical absorption via surface plasmon excitation in metal nanoparticles. Appl Phys Lett 86:063106/1-3. doi:10.1063/1.1855423

Shankar SS, Rai A, Ankamwar B, Singh A, Ahmad A, Sastry M (2004) Biological synthesis of triangular gold nanoprisms. Nat Mater 3:482–488. doi:10.1038/nmat1152

Shuford KL, Ratner MA, Schatz GC (2005) Multipolar excitation in triangular nanoprisms. J Chem Phys 123:1147131/1-9. doi:10.1063/1.2046633

Tsuji M, Miyamae N, Lim S, Kimura K, Zhang X, Hikino S, Nishio M (2006) Crystal structures and growth mechanisms of Au@Ag core-shell nanoparticles prepared by the microwave-polyol method. Cryst Growth Des 6:1801–1807. doi:10.1021/cg060103e

Tsutsui Y, Hayakawa T, Kawamura G, Nogami M (2011) Tuned longitudinal surface plasmon resonance and third-order nonlinear optical properties of gold nanorods. Nanotechnology 22:275203/1-7. doi:10.1088/0957-4484/22/27/275203

Wang Y, Schlucker S (2013) Rational design and synthesis of SERS label. Analyst 138:2224–2238. doi:10.1039/C3AN36866A

Xu S, Cao Y, Zhou J, Wang X, Wang X, Xu W (2011) Plasmonic enhancement of fluorescence on silver nanoparticle films. Nanotechnology 22:275725/1-7. doi:10.1088/0957-4484/22/27/275715

Yamaguchi K, Inoue T, Fujii M, Ogawa T, Matsuzaki Y, Okamoto T, Haraguchi M (2007) Characteristics of light intensity enhancement of a silver nanoprism with rounded corners. J Microsc 229:545–550. doi:10.1111/j.1365-2818.2008.01941.x

Yang P, Portales H, Pileni MP (2009) Identification of multipolar surface plasmon resonances in triangular silver nanoprisms with very high aspect ratios using the DDA method. J Chem Phys C 113:11597–11604. doi:10.1021/jp901248e

Young KL, Jones MR, Zhang J, Macfarlane RJ, Esquivel-Sirvent R, Nap RJ, Wu J, Schatz GC, Lee B, Mirkin CA (2012) Assembly of reconfigurable one-dimensional colloidal superlattices due to a synergy of fundamental nanoscale forces. Proc Natl Acad Sci 109:2240–2245. doi:10.1073/pnas.1119301109